Reactivity of Zinc Halide Complexes Containing Camphor-Derived Guanidine Ligands with Technical *rac*-Lactide

Angela Metz [1], Joshua Heck [1], Clara Marie Gohlke [1], Konstantin Kröckert [1], Yannik Louven [1], Paul McKeown [2], Alexander Hoffmann [1], Matthew D. Jones [2] and Sonja Herres-Pawlis [1,*] [iD]

[1] Institute of Inorganic Chemistry, RWTH Aachen University, Landoltweg 1, 52074 Aachen, Germany; angela.metz@ac.rwth-aachen.de (A.M.); joshua.heck@rwth-aachen.de (J.H.); marie.gohlke@rwth-aachen.de (C.M.G.); konstantin.kroeckert@rwth-aachen.de (K.K.); yannik.louven@rwth-aachen.de (Y.L.); alexander.hoffmann@ac.rwth-aachen.de (A.H.)

[2] Centre for Sustainable Chemical Technologies, Department of Chemistry, University of Bath, Claverton Down, Bath BA2 7AY, UK; p.mckeown@bath.ac.uk (P.M.); M.Jones2@bath.ac.uk (M.D.J.)

* Correspondence: sonja.herres-pawlis@ac.rwth-aachen.de; Tel.: +49-241-80-939-02

Abstract: Three new zinc complexes with monoamine–guanidine hybridligands have been prepared, characterized by X-ray crystallography and NMR spectroscopy, and tested in the solvent-free ring-opening polymerization of *rac*-lactide. Initially the ligands were synthesized from camphoric acid to obtain TMGca and DMEGca and then reacted with zinc(II) halides to form zinc complexes. All complexes have a distorted tetrahedral coordination. They were utilized as catalysts in the solvent-free polymerization of technical *rac*-lactide at 150 °C. Colorless polylactide (PLA) can be produced and after 2 h conversion up to 60% was reached. Furthermore, one zinc chlorido complex was tested with different qualities of lactide (technical and recrystallized) and with/without the addition of benzyl alcohol as a co-initiator. The kinetics were monitored by in situ FT-IR or ^{1}H NMR spectroscopy. All kinetic measurements show first-order behavior with respect to lactide. The influence of the chiral complexes on the stereocontrol of PLA was examined. Moreover, with MALDI-ToF measurements the end-group of the obtained polymer was determined. DFT and NBO calculations give further insight into the coordination properties. All in all, these systems are robust against impurities and water in the lactide monomer and show great catalytic activity in the ROP of lactide.

Keywords: ring-opening polymerization; polylactide; zinc; guanidine

1. Introduction

Due to increasing environmental awareness, plastics based on petrochemical resources have to be replaced by plastics based on renewable raw materials. Nowadays several polymers, such as starch plastics, polyhydroxyalkanoate (PHA), cellulose acetate, and polylactide (PLA), can be used as an alternative to petrochemical-based plastics [1–5]. PLA has the greatest potential. Due to its resemblance to petrochemical polymers, PLA is utilized in the medical field, packaging, and microelectronics [5–9]. It is a biodegradable and biocompatible aliphatic polyester that can be produced from renewable raw materials such as corn and sugar beets [3,4,6–16]. PLA is produced by the ring-opening polymerization (ROP) of lactide, the dimer of lactic acid, using a metal-based catalyst system. For a broad application field, high molar masses, low dispersity values, and a control over the tacticity of the resulting PLA are key features [6–9,13]. The tacticity can be influenced by three parameters: polymer chain end, ligand chirality, and solvent [17–28]. Most catalysts produce atactic or heterotactic PLA but with isotactic PLA

the mechanical strength, melting point, and physical properties can be enhanced [29]. It is desirable to synthesize new catalysts that satisfy these requirements.

In recent decades, numerous catalysts based on tin, zinc, aluminium, rare earth metals, and titanium containing anionic ligand systems were investigated. These ligand systems were used: trispyrazolylborates [30,31], aminophenolates [32], β-ketiminates [33–41], salan/salalen ligands, and Schiff bases [23–28,42–46], as well as alkyl ligands derived from acids [47]. Jones and co-workers synthesized bipyrrolidine salan proligands containing as the metal center Zr^{IV}, Ti^{IV}, Hf^{IV}, and Al^{III}, which show high activity and control on the tacticity [42–44]. The fastest systems could be obtained by Williams et al. These dizinc complex systems containing Schiff bases can polymerize lactide at room temperature within one minute and without the addition of a co-initiator [48,49]. The problem with these anionic ligand systems is that the polymerization has mostly be enperformed with purified lactide (several times recrystallized or sublimed) and in solution, which is not suitable for industrial applications. Moreover, the catalysts are often combined with a high sensitivity towards moisture, air, and lactide impurities. Due to these conditions, the industrial target is to synthesize stable systems that can polymerize technical lactide under bulk conditions. Nowadays, the commonly used catalyst is tin(II) 2-ethylhexanoate, with alcohols as the initiating species [50–52]. Here the problem is the toxicity of the tin that remains in the polymers and, after composting, accumulates in the environment [53]. Feijen et al. published some criteria that an industrially used catalyst should meet. In addition, the ligands should be cheap and commercially available, the complex must be synthesized in high yields, the activity in the ROP (bulk conditions) is important, and the obtained polymer must be colorless with high molar masses [19]. A promising alternative is zinc containing neutral ligands as it is non-toxic, cost-efficient, robust against lactide impurities and water, and shows high activity. A large variety of neutral ligand systems are well-known, e.g., phosphinimines [54–58], iminopyridines [59,60], trispyrazolylmethanes [61], carbenes [62,63], piperidinyl-benzyl-anilines [64], and guanidine systems [65–68].

Jeong and co-workers synthesized in situ diisopropoxide zinc complexes with camphorylimine and produced heterotactic-enriched PLA with a narrow dispersity and good control at 25 °C in THF [59,60]. A low dispersity and very fast polymerization in bulk or solution were achieved with carbene zinc complexes by Tolman et al. The problem with this is that only purified lactide was used [62,63]. Superior robustness for lactide polymerization can be achieved with zinc guanidine complexes. As an example, zinc hybridguanidine/bisguanidine complexes show high activity in bulk and with technical *rac*-lactide at 150 °C [69,70]. Moreover, great activity can be reached with robust zinc complexes containing N,O donor functionalities [71]. With quinoline–guanidine bis(chelate) triflato complexes high activity with technical lactide and good molar masses can be reached. However, the comparable zinc chlorido complexes did not show any activity [72–74].

Herein, we report the synthesis and the full characterization of three new chiral monoamine-guanidine hybrid zinc complexes. As starting material, camphoric acid was used. These complexes were tested in the solvent-free polymerization of *rac*-lactide at 140 °C or 150 °C with or without a co-initiator. All complexes show high activity in the ROP of lactide and produce a polymer in a very short reaction time. DFT and NBO calculations were performed to obtain insight into the coordination properties. These systems provide an excellent, sustainable alternative to commercially used tin complexes.

2. Results and Discussion

2.1. Zinc Halide Complexes

One new monoamine-hybridguanidine ligand 3-((1,3-dimethylimidazolidine-2-ylidene)amino)-1, 2,2-trimethylcyclopentane-1-amine (DMEGca) and the recently published ligand 2-(3-amino-2,2,3-trimethylcyclopentyl)- 1,1,3,3-tetramethylguanidine (TMGca) [75] based on camphoric acid were prepared by the reaction of the corresponding Vilsmeier salt *N,N'*-dimethylethylenechl

oroformamidiniumchloride or *N,N,N′,N′*-tetramethyl-chloroformamidiniumchloride with the diamine [76,77]. First the (1*R*, 3*S*)-camphor-bisamine has to be generated on the basis of (1*R*, 3*S*)-camphor acid via a Curtius rearrangement [75]. The addition of one equivalent of Vilsmeier salt and the presence of trimethylamine leads to the monoamine-guanidine hybridligands **L1** (TMGca) and **L2** (DMEGca) [76,77] (Figure 1).

TMGca, **L1**   DMEGca, **L2**
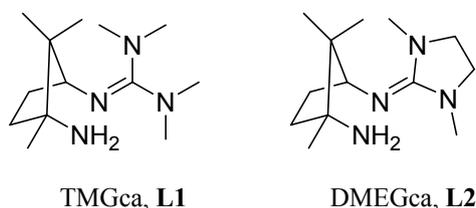
Figure 1. Overview of the utilized monoamine-guanidine hybridligands **L1** [75] and **L2**.

The ligands were used in complex synthesis with anhydrous zinc chloride/bromide in dry THF to obtain crystals suitable for X-ray crystallography (Figure 2). Three zinc halide complexes, **C1** [Zn(TMGca)Cl$_2$], **C2** [Zn(DMEGca)Cl$_2$], and **C3** [Zn(DMEGca)Br$_2$], were obtained. In all complex systems, two molecules are in the asymmetrical unit. Since both conformers show similar bond lengths and angles, only one was used for more precise examinations. In Table 1 the bond lengths and angles of these complexes are summarized. The zinc atom is fourfold coordinated by one primary amine, one guanidine moiety, and two halide atoms. Due to the different coordination strength, the bond lengths for Zn–N$_{gua}$ (1.986(3), 2.013(4), 2.065(5) Å) are shorter than for Zn–N$_{amine}$ (2.053(3), 2.065(4), 2.041(5) Å). This trend can be seen in recent studies [69,78]. The angle of ZnN$_2$ is around 100° and the angle between the coordination planes {∡ (ZnX$_2$, ZnN$_2$)} is 80.3°–83.4°, in good agreement with the value expected for an ideal tetrahedral geometry of 90°. All complexes are tetrahedrally distorted coordinated, which can be shown by the structural parameter τ_4. A value of 0 indicates a square-planar coordination, whereas a value close to 1 indicates a tetrahedral environment [79]. In all complexes the τ_4-value is between 0.87 and 0.89. The delocalization of the guanidine double bond is best described by the structural parameter ρ [80]. A value of 1 shows a completely delocalization. The value could be determined by the ratio of the C$_{gua}$–N$_{gua}$ bond length to the sum of the C$_{gua}$–N$_{amine}$ bond. For all complexes the value is 0.96/0.97, which shows moderate delocalization. The intraguanidine twist is defined as the angles between the planes of N$_{gua}$–N$_{amine}$–N$_{amine}$ and C$_{gua}$–C$_{amine}$–C$_{amine}$. In **C1** the averaged angle lies in the region of 35.6°, whereas in **C2** and **C3** the value is 13.1° and 7.1°. In **C2** and **C3** the free rotation in the guanidine moiety is hindered, which leads to smaller angles [69–71]. All complexes were fully identified by NMR, IR spectroscopy, and MS measurements. They are stable under air and do not hydrolyze.
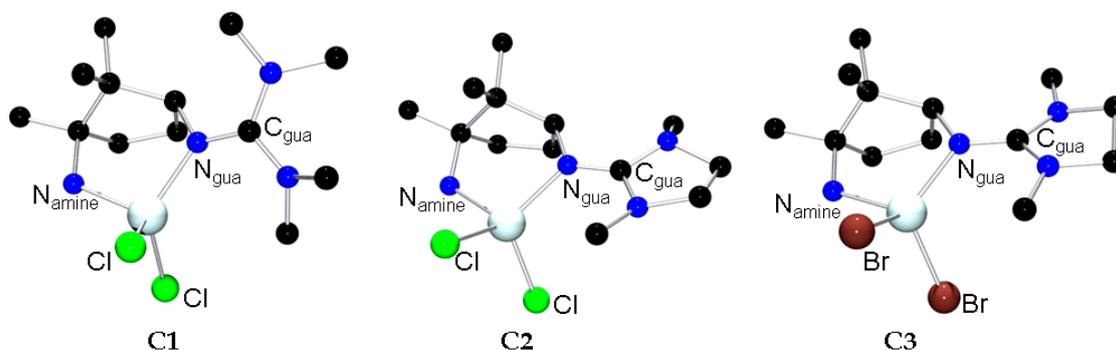
Figure 2. Molecular structures in the solid state of **C1**–**C3**. H atoms are omitted for clarity.

Table 1. Key bond lengths and angles of the zinc complexes **C1** [Zn(TMGca)Cl$_2$], **C2** [Zn(DMEGca)Cl$_2$], and **C3** [Zn(DMEGca)Br$_2$].

	C1	**C2**	**C3**
Zn–N$_{gua}$ [Å]	1.986(3)	2.013(4)	2.006(5)
Zn–N$_{amine}$ [Å]	2.053(3)	2.065(4)	2.041(5)
Zn–X [Å]	2.246(2), 2.284(2)	2.261(2), 2.292(2)	2.395(2), 2.434(2)
N$_{amine}$–Zn–N$_{gua}$ [°]	99.8(2)	100.3(2)	101.2(2)
∡ (ZnCl$_2$, ZnN$_2$) [°]	80.3	80.6	83.4
τ_4 [a]	0.89	0.88	0.87
ρ [b]	0.97	0.96	0.97
Guanidine twist [c]	35.6	13.1	7.1

[a] $\tau_4 = \frac{360° - (\alpha + \beta)}{141°}$ α, β = largest angles around metal centre [79]; [b] $\rho = \frac{2a}{(b+c)}$ with a = d(C$_{gua}$–N$_{gua}$) and b and c = d(C$_{gua}$–N$_{amine}$) [80]; [c] The dihedral angles between the planes represented by N$_{gua}$, N$_{amine}$, N$_{amine}$ and C$_{gua}$, C$_{Alk}$, C$_{Alk}$. Two twist angles for each guanidine moiety. Average value of dihedral angles.

2.2. Density Functional Theory Calculations

The electronic structures of the complexes can be modeled by DFT calculations to obtain more precise insights into the donor properties of the ligands. A benchmark of similar complexes was performed in earlier reports [69]. All studies were performed by DFT with the functional TPSSh [81], def2-TZVP [82] as basis set, and empirical dispersion correction with Becke–Johnson damping GD3BJ [83–85] in the solvent acetonitrile (as SMD model). The results are shown in Table 2. The bond lengths are predicted to be longer than the experimental values, although the relative trend is well reproduced. The bond angles and structural parameter τ_4 and ρ are in good agreement with the values obtained from the crystal structures. The DFT calculations show as well as before that the guanidine nitrogen atoms lead to shorter Zn–N$_{gua}$ bond lengths, which shows the stronger donor strength in comparison to the N$_{amine}$ atom.

Table 2. Calculated bond lengths [Å] and angles [°] of **C1**–**C3** [Gaussian09, TPSSh, def2-TZVP, GD3BJ, SMD:MeCN].

	C1	**C2**	**C3**
Zn–N$_{gua}$	2.009	2.053	2.024
Zn–N$_{amine}$	2.080	2.105	2.093
Zn–X	2.302, 2.314	2.303, 2.345	2.425, 2.430
N$_{amine}$ZnN$_{gua}$	99.3	97.9	99.1
∡ (ZnX$_2$, ZnN$_2$)	83.5	75.3	88.7
τ_4 [a]	0.86	0.81	0.89
ρ [b]	0.97	0.95	0.96
Guanidine twist [c]	35.6	14.5	6.2

[a] $\tau_4 = \frac{360° - (\alpha + \beta)}{141°}$ α, β = largest angles around metal centre [79]; [b] $\rho = \frac{2a}{(b+c)}$ with a = d(C$_{gua}$–N$_{gua}$) and b and c = d(C$_{gua}$–N$_{amine}$) [80]; [c] The dihedral angles between the planes represented by N$_{gua}$, N$_{amine}$, N$_{amine}$ and C$_{gua}$, C$_{Alk}$, C$_{Alk}$. Two twist angles for each guanidine moiety. Average value of dihedral angles.

To get better insights into the donor–acceptor interactions of the complexes, NBO (natural population analysis) calculations were performed. The optimized structures obtained were used to calculate the charge transfer energies (by second-order perturbation theory) and the NBO charges [86–88]. Normally, these two sets of computed values allow an estimation of the relative donor strength [78]. The influence of the electronic effects can be reflected well by the NBO charges, but these do not represent absolute charges. In Table 3 the NBO charges on Zn, N$_{amine}$, and N$_{gua}$ are depicted. The calculated charges on the zinc atoms lie in the range of 1.49–1.56 and the donating nitrogen atoms of the primary amines have very strong negative charges (−0.95), whereas the charges of the nitrogen atoms of the guanidine moiety are between (−0.76) and (−0.79). The N$_{gua}$ atom appears less basic than the N$_{amine}$ atoms. This is in contrast to previous studies, where the N$_{gua}$ donor is more

basic and the stronger donor when compared to amine donors [69]. In all complexes, the Zn–N bonds were identified by NBO as covalent bonds; hence, no donor–acceptor interaction energies could be obtained. Together with the short Zn–N_{gua} bonds, the picture seems mixed: guanidines are strong donors AND highly basic, but here, NBO predicts that amine will be more basic. Hence, in this case, the DFT analysis does not help elucidate the question of the donor strength. Further studies on amine–guanidine complexes are needed in the future.

Table 3. Natural charge on zinc, N_{gua}, N_{amine}, and halide atoms for complexes **C1–C3**.

	C1	**C2**	**C3**
Zn	1.56	1.56	1.49
N_{amine}	−0.95	−0.95	−0.95
N_{gua}	−0.78	−0.76	−0.79
Cl/Br	−0.85/−0.85	−0.85/−0.85	−0.81/−0.81

2.3. Polymerization Experiments

Initially, complexes **C1–C3** were tested in the activity of the ring-opening polymerization of technical, unsublimed *rac*-lactide under bulk conditions without any co-initiator at 150 °C (polymerization method **a**, Scheme 1, Table 4). The use of technical lactide and the high temperatures should reflect the industrial relevant conditions [9]. The start of the measurement is when the lactide monomer was melted. With one chlorido complex, two more kinetic measurements at 140 °C under stirring (400 rpm) were carried out (polymerization method **b** and **c**) (Table 4). Benzyl alcohol was added to one polymerization to determine if it can open the ring of the lactide monomer and to see the impact on the molar masses (polymerization method **c**) (Table 4). In recent reports [70] it could be shown that the quality of lactide (technical or recrystallized) has no major impact on the activity of the polymerization. As a result, in polymerization methods **b** and **c** different qualities of lactide are used (Table 4). More details for the individual measurements are shown below (Table 4). After each measurement the conversion was determined by ^{1}H NMR or FT-IR spectroscopy and the molar mass and dispersity D have been measured by GPC (gel permeation chromatography). The reaction constant k_{app} equals the slope of the linear fit of the semilogarithmic plot of the concentration against time. The technical lactide was stored at −33 °C in a glove box to guarantee the same conditions at every measurement. Every measurement has been performed at least twice.
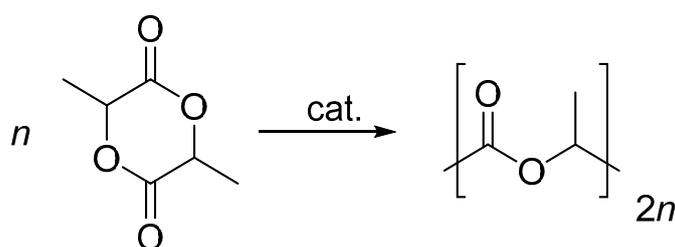
Scheme 1. ROP of lactide.

Table 4. Polymerization conditions for polymerization methods **a–c**.

Polymerization Method	Ratio (Monomer:Catalyst:Initiator)	Reaction Temperature (°C)	Stirring (rpm)	Quality *rac*-Lactide	Conversion Determination
a	500:1:0	150	-	technical	^{1}H NMR
b	1000:1:0	140	400	technical	^{1}H NMR
c	1000:1:10	140	400	recrystallized	FT-IR

Polymerization method **a** has been conducted in an oven at 150 °C. First 180–200 mg of finely crushed monomer:catalyst (500:1) were weighed in a 2-mL reaction vessel and sealed under nitrogen. The reaction time was up to 6 h. Figure 3 shows the first-order controlled polymerization catalyzed by the zinc halide complexes **C1**–**C3**. All complexes show high activity at $k_{app} = (7.3–12.8) \times 10^{-5}$ s^{-1}. Complex **C3** with bromide as halide showed the fastest reactivity for the ROP of lactide ($k_{app} = 12.8 \times 10^{-5}$ s^{-1}) (Figure 3 and Table 5). After 2 h a conversion of more than 50% can be reached. It has to be noted that the conversion for **C1** and **C3** seems very similar after 2 h, which is related to the non-zero intercept of the kinetics for **C1**. This intercept may be due to initiation by additional water molecules from the technical lactide. The bridging unit in the guanidine group has no influence on the polymerization activity. All in all, all three catalysts polymerize in the similar range of k_{app}. They show similar reaction times. The obtained colorless polymers have a chain length between 5000 and 20,000 g/mol, which is shorter than the calculated molar masses. The use of technical lactide leads to more short chains due to the residual water and other impurities, which leads to chain transfer reactions. Also, intra- and intermolecular transesterification events lead to shorter chains than expected [4].
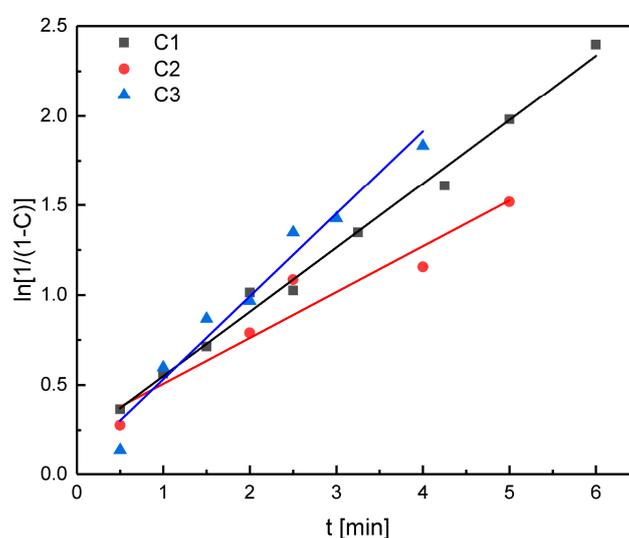
Figure 3. Semilogarithmic plot of the polymerization of technical *rac*-lactide [LA]:[catalyst] = 500:1, $T = 150$ °C, conversion determined via ^{1}H NMR spectroscopy.

Table 5. Polymerization data from polymerization method **a** for complexes **C1**–**C3** after two hours.

	k_{app} [a] $(10^{-5}$ s$^{-1})$	Conversion (%) [b]	$M_{n,exp}$ (g/mol) [c]	$M_{n,calcd.}$ (g/mol)	Đ [c]	P_r [d]
C1	9.9	64	20,000	46,000	1.70	0.58
C2	7.3	55	5100	39,500	1.72	0.56
C3	12.8	62	13,000	44,500	1.74	0.54

Conditions: two hours, [M]/[Cat] = 500/1, 150 °C, solvent free, technical *rac*-lactide. [a] Determined from the slope of the plots of ln(1/(1 − C)) versus time; [b] Determined by integration of the methine region of the ^{1}H NMR spectrum; [c] Determined by gel permeation chromatography (GPC) in THF using a viscosimetry detector; [d] Probability of racemic enchainment calculated by analysis of the homonuclear decoupled ^{1}H NMR spectra [31,33].

To check the impact of the chirality of the complexes on the tacticity of the polymer, homonuclear decoupled ^{1}H NMR spectra were measured for the resulting polymers [31,33]. The probability value of the heterotactic enchainment P_r is between 0.54 and 0.58 for all complexes, which shows an atactic polymer with a very slight heterotactic bias (Table 5). One reason why the chiral complexes have no

influence on the stereocontrol of the polymerization is that the stereo information is not transferred to the polymer due to a lack of steric encumbrance at high temperatures.

Moreover, with **C2** further investigations were performed in an oil bath (polymerization method **b**) and in a jacketed vessel (polymerization method **c**). The reason why we have chosen **C2** for more investigations is that all catalysts show similar reaction constants in polymerization and a higher yield can be obtained for **C2** (which is important for industrial use). The ratio was 1000:1 (polymerization method **b**) and 1000:1:10 (BzOH) (polymerization method **c**) to determine the impact of the addition of benzyl alcohol on the polymerization activity. The reaction temperature was 140 °C, stirring speed 400 rpm, and in polymerization method **c** an IR spectra was recorded every 5 min. The final reaction time in **b** was 13 h and in **c** 7 h. In polymerization method **b** technical lactide was used and in polymerization method **c** recrystallized lactide was used. In a recently published study it was shown that the quality of recrystallized vs. technical lactide makes no difference for our systems [70]. The conversion in polymerization method **b** was determined via ^{1}H NMR spectroscopy and in polymerization method **c** with FT-IR spectroscopy. Here, the area between 1260 cm^{-1} and 1160 cm^{-1} shows the C–O–C stretch of the lactide monomer and the C–O–C asymmetric vibrations in the polymer chain of the polylactide (Figure 4) [89]. After integration over these two regions, the conversion can be determined. In the recent study we could show that the two different setups (oil bath: conversion determined by ^{1}H NMR spectroscopy (polymerization method **b**) or jacketed vessel: conversion determined by FT-IR spectroscopy (polymerization method **c**) make no difference to the polymerization activity and reaction constant [70].
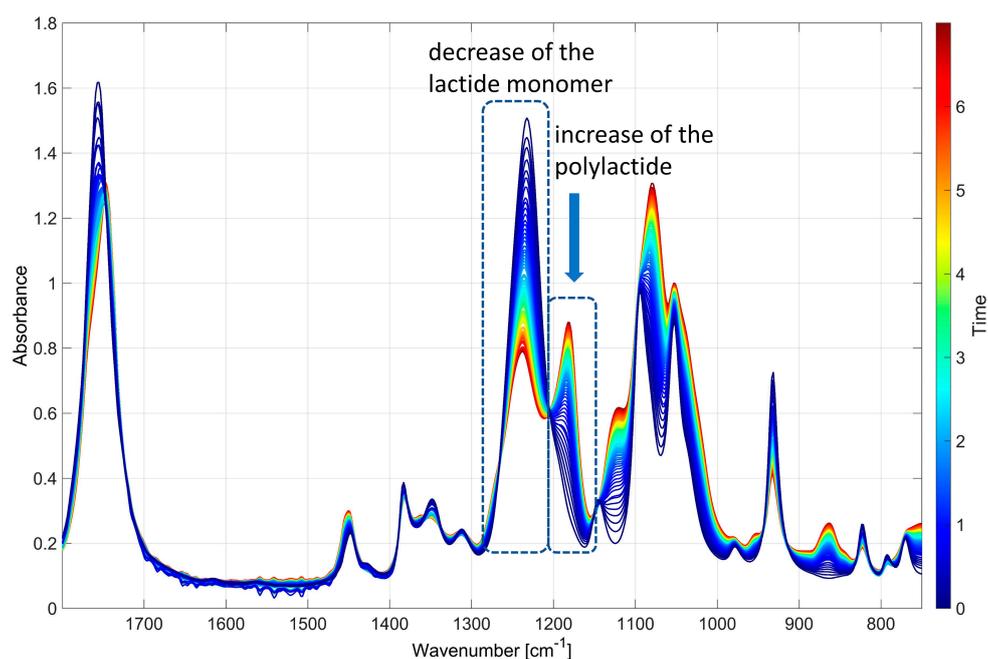
Figure 4. 2D time-resolved FT-IR spectra of the polymerization method **c** *rac*-lactide with **C2**.

The polymerization with benzyl alcohol is more than three times faster than without (Table 6 and Figure 5). After 7 h a conversion, determined by ^{1}H NMR spectroscopy up to 65% in polymerization method **c** can be obtained, whereas in polymerization method **b** after 13 h only 66% can be determined. The molar masses were determined after 7 h (polymerization method **c**, M_n = 8000 g/mol) and are in good accordance with the theoretical ones (9400 g/mol). The dispersity of 1.15 shows excellent control for polymerization method **c**. Kinetic investigations for polymerization method **b** show it does not pass through the origin. The reason could be the additional initiating systems (e.g., water and impurities in the lactide monomer), which lead to faster polymerization in the beginning. The molar masses in

polymerization method **b** of 56,000 g/mol are too low (expected M_n = 91,000 g/mol). One reason could be the additional water residues in the technical lactide monomer. Presumably the recrystallized lactide still has some water residues. The Đ value of 1.57 shows good reaction control.

To obtain some insight into the mechanism of the polymerization, end-group analyses were performed with MALDI-ToF measurements. The MALDI-ToF measurements for the polymerization with the co-initiator benzyl alcohol reveal benzyl alcohol at the end of the chain. It can be shown that in polymerization **c** a low degree of transesterification is obtained. Ethoxy and OH$^-$ are the end group of the polymerization without benzyl alcohol. The ethoxy end group stems from the precipitation of the polymer in ethanol and the water residue is due to the technical lactide monomer (see Figures S1 and S2). The exact mechanism of these complex systems is not yet known. The complexes do not act as a single-site catalyst since they cannot open the lactide monomer themselves. As initiating systems, a co-initiator, which can be benzyl alcohol or water, has the task of starting the polymerization catalyzed by the zinc guanidine complexes. In comparison to other zinc *N,N*-guanidine complexes, these systems show by far the highest activity in polymerization [65,69,70,72]. N_{gua},O zinc chlorido complexes show the same reaction constants but yield polymers with molar masses, in good accordance with the theoretical ones, which demonstrates excellent reaction control [71].

Table 6. Reaction constants for varying polymerization conditions with **C2**.

Polymerization Method	k_{app} [a] (10^{-5} s^{-1})	C (%) [b]	$M_{n,exp.}$ (g/mol) [c]	$M_{n,calcd.}$ (g/mol)	Đ [c]
b	1.4	63 (after 13 h)	56,000 (after 13 h)	91,000	1.57 (after 13 h)
c	4.8	65 (after 7 h)	8000 (after 7 h)	9400	1.15 (after 7 h)

[a] Determined from the slope of the plots of ln(1/(1 − C)) versus time; [b] Determined by ^{1}H NMR spectroscopy; [c] Determined by gel permeation chromatography (GPC) in THF using a viscosimetry detector.
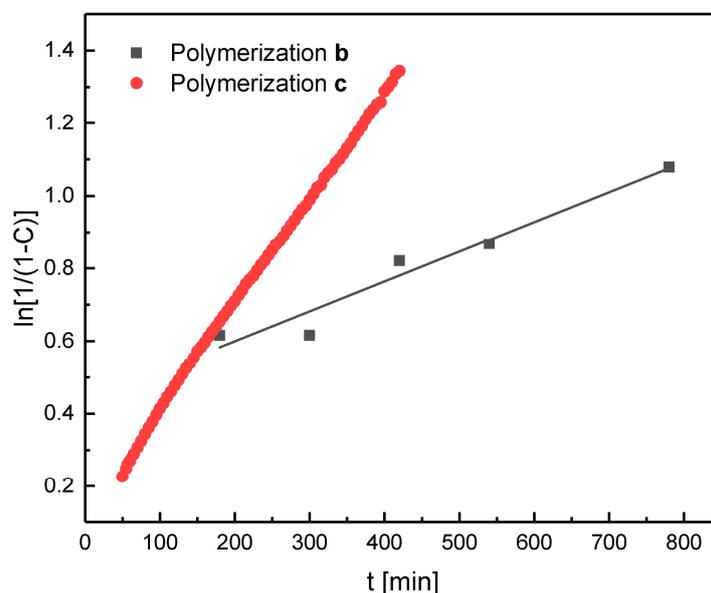
Figure 5. Polymerization method **b** and **c** with **C2** at 140 °C, 400 rpm. **b** = 1000:1, technical *rac*-lactide. **c** = 1000:1:10, recrystallized *rac*-lactide.

3. Materials and Methods

All steps were performed under nitrogen (99.996%) dried with P_4O_{10} granulate using Schlenk techniques. Solvents were purified according to literature procedures and also kept under nitrogen [90]. All chemicals were purchased from Sigma-Aldrich GmbH (Taufkirchen, Germany), TCI GmbH (Eschborn, Germany) and ABCR GmbH (Karlsruhe, Germany) and were used as received without further purification.

D,L-lactide (Total Corbion) was stored at −33 °C under an inert atmosphere in a glove box. The precursors of the ligands TMGca and DMEGca were synthesized from (1*R*, 3*S*)-(+)-camphoric acid [75]. Ligand **L1** was synthesized according to the literature [75]. *N*,*N*′-dimethylethylenechloroformamidinium chloride (DMEG-VS) and *N*,*N*,*N*′,*N*′-tetramethylchloroformamidinium chloride (TMG-VS) were synthesized as described in the literature [76,77].

3.1. Physical Methods

For **L2** mass spectrum was obtained with a ThermoFisher Scientific Finnigan MAT 95 mass spectrometer (Waltham, MA, USA) for HR-EI and for **C1**–**C3** a ThermoFisher Scientific LTQ-Orbitrap XLSpectrometer for HR-ESI. The tube lens voltage lay between 100 and 130 V.

FT-IR spectra were measured with a Thermo Scientific Nicolet Avatar 380 spectrometer as KBr pellets (**C1**–**C3**) or as film between NaCl plates (**L2**).

NMR spectra were recorded on the following spectrometers: Bruker (Karlsruhe, Germany) Avance II (400 MHz) or Bruker Avance III (400 MHz) (**L2**, **C1**–**C3**). The NMR signals were calibrated to the residual signals of the deuterated solvent (δ_H(CDCl$_3$) = 7.26 ppm).

MALDI-ToF mass spectra were determined on a Bruker Autoflex speed instrument using DCTB (*trans*-2-[3-(4-*tert*-Butylphenyl)-2-methyl-2-propenylidene]malonitrile) as matrix and ionized with sodium trifluoroacetate. Spectra were measured in reflector-positive mode.

Gel Permeation Chromatography (GPC): The average molar masses and the mass distributions of the obtained polylactide samples of polymerization **a**,**b** were determined by gel permeation chromatography (GPC) in THF as mobile phase at a flow rate of 1 mL/min at 35 °C. The utilized GPCmax VE-2001 from Viscotek (Waghausel-Kirrlach, Germany) is a combination of an HPLC pump, two Malvern Viscotek T columns (porous styrene divinylbenzene copolymer) with a maximum pore size of 500–5000 Å, a refractive indaex detector (VE-3580), and a viscometer (Viscotek 270 Dual Detector). Universal calibration was applied to evaluate the chromatographic results. GPC analysis of polymerization **c** was carried out on an Agilent 1260 GPC/SEC MDS (Santa Clara, CA, USA) equipped with two PL MixedD 300 × 7.5 mm columns and a guard column, all heated to 35 °C. THF was used as eluent at a flow rate of 1 mL/min. A refractive index (RI) detector was used and this was maintained at 35 °C and referenced to 11 narrow polystyrene standards.

3.2. X-ray Analyses

The single crystal diffraction data for **C1**–**C3** are presented in Table 7. These data were collected on a Bruker D8 goniometer with APEX CCD detector. An Incoatec microsource with Mo-Kα radiation (λ = 0.71073 Å) was used and temperature control was achieved with an Oxford Cryostream 700. Crystals were mounted with grease on glass fibers and data were collected at 100 K in ω-scan mode. Data were integrated with SAINT [91] and corrected for absorption by multi-scan methods with SADABS [92]. The structure was solved by direct and conventional Fourier methods and all non-hydrogen atoms were refined anisotropically with full-matrix least-squares based on F^2 (XPREP [93], *SHELXS* [94] and ShelXle [95]). Hydrogen atoms were derived from difference Fourier maps and placed at idealized positions, riding on their parent C atoms, with isotropic displacement parameters Uiso(H) = 1.2Ueq(C) and 1.5Ueq(C methyl). All methyl groups were allowed to rotate but not to tip. Full crystallographic data (excluding structure factors) have been deposited with the Cambridge Crystallographic Data Centre as supplementary no. CCDC–1579451 for **C1**, CCDC–1579452 for **C2** and CCDC–1579453 for **C3**. Copies of the data can be obtained free of charge on application to CCDC, 12 Union Road, Cambridge CB2 1EZ, UK (fax: (+44)-1223-336-033; e-mail: deposit@ccdc.cam.ac.uk).

Important crystallographic information on **C1**–**C3** is shown in Table 7.

Table 7. Crystallographic data and parameters for **C1**–**C3**.

	C1	C2	C3
Empirical formula	$C_{13}H_{28}Cl_2N_4Zn$	$C_{13}H_{26}Cl_2N_4Zn$	$C_{13}H_{26}Br_2N_4Zn$
Formula mass (g·mol^{-1})	376.66	374.65	463.57
Crystal size (mm)	$0.24 \times 0.21 \times 0.18$	$0.23 \times 0.16 \times 0.16$	$0.23 \times 0.20 \times 0.19$
T (K)	100(2)	100(2)	100(2)
Crystal system	Orthorhombic	Monoclinic	Monoclinic
Space group	$P2_12_12_1$	$P2_1$	$P2_1$
a (Å)	13.478(2)	9.472(2)	9.297(2)
b (Å)	15.173(2)	18.095(3)	14.257(3)
c (Å)	17.570(2)	10.133(2)	13.200(3)
α (°)	90	90	90
β (°)	90	103.91(1)	101.84(1)
γ (°)	90	90	90
V (Å^3)	3593.1(8)	1685.8(5)	1712.4(6)
Z	8	4	4
$\rho_{calcd.}$ (Mg·m^{-3})	1.393	1.476	1.798
μ (mm^{-1})	1.661	1.770	6.098
λ (Å)	0.71073	0.71073	0.71073
$F(000)$	1584	784	928
hkl range	$-17 \leq h \leq 12, \pm 20,$ $-23 \leq l \leq 22$	$\pm 12, \pm 24, \pm 13$	$\pm 11, \pm 17, \pm 16$
Reflections collected	28,044	17,928	20,541
Independent reflections	8953	8244	7045
$R_{int.}$	0.0776	0.0556	0.0516
Number of parameters	391	387	385
R_1 $[I \geq 2\sigma(I)]$	0.0438	0.0434	0.0455
wR_2 (all data)	0.0942	0.0942	0.1164
Goodness-of-fit	0.946	0.985	1.027
Largest diff. peak, hole [eÅ^{-3}]	0.420, -0.413	0.449, -0.427	1.989, -1.153
Absolute structure parameter	0.013(10)	0.000(13)	0.009(13)

3.3. Computational Details

Density functional theory (DFT) calculations were performed with the program suite Gaussian 09 rev. E.01 [96]. The starting geometries for all complexes were generated from the molecular structures from the X-ray crystallography data. The Gaussian 09 calculations are performed with the nonlocal hybrid meta GGA TPSSh functional [83–85] and with the Ahlrichs type basis set def2-TZVP [82]. As solvent model, we used the SMD Model (SMD, acetonitrile) [97] as implemented in Gaussian 09. As empirical dispersion correction, we used the D3 dispersion with Becke–Johnson damping, as implemented in Gaussian, Revision E.01 [84,85]. For TPSSh, the values of the original paper have been substituted by the corrected values kindly provided by S. Grimme as private communication [83]. NBO calculations were accomplished using the program suite NBO 6.0 [86–88]. Some of these calculations have been performed within the MoSGrid environment [98–100].

3.4. Polymerization

All polymerizations were reproduced at least twice.

For polymerization **a**, the reaction vessels were prepared in a glove box and the technical lactide was stored at -33 °C in a glove box. The lactide and the catalyst (500:1) were weighed separately and homogenized in an agate mortar. The reaction mixture was placed in 10 reaction vessels (180–200 mg), tightly sealed and heated at 150 °C outside the glove box. The same applies for polymerization **b**. The ratio was 1000:1. In seven Young flasks 0.5 g of the mixture was added. The tubes, containing a stirring bar (stirring speed = 400 rpm), were heated in an oil bath to 140 °C. The polymerization started with the melting point. After stopping the reaction under cool water the conversion was determined by dissolving the sample in 1–2 mL DCM and a ^{1}H NMR spectrum was taken. The PLA was precipitated in ethanol (150 mL) and dried at 50 °C.

Polymerization kinetics followed by FT-IR spectroscopy (polymerization **c**) were measured with a Bruker Matrix-MF FT-IR spectrometer equipped with a diamond ATR probe (IN350 T) suitable for Mid-IR in situ reaction monitoring. The kinetics were carried out in a jacketed vessel under Argon counterflow and stirring conditions (mechanical stirring system 400 rpm), and the vessel was connected to a Huber Petite Fleur-NR circulation thermostat to keep the temperature constant (adjusted temperature: 150 °C; reaction temperature: 140 °C). After heating the recrystallized *rac*-lactide (0.14 mol) to 140 °C, a background spectrum was recorded before the IR probe was placed in the lactide melt. Subsequently the catalyst (1.39×10^{-4} mol) and the benzyl alcohol (1.39×10^{-3} mol) were added under argon to the lactide melt. A measurement was recorded every five minutes to see the decrease of the C–O–C lactide monomer peak against the increase of the C–O–C asymmetric vibrations of the polylactide in the IR spectrum [89]. The evaluating software was OPUS (Bruker Optik GmbH 2014).

3.5. General Synthesis of Bisguanidine Ligands with Chloroformamidinium Chlorides

The corresponding primary diamine (4.26 g, 30 mmol) and triethylamine (3.03 g, 30 mmol) were dissolved in acetonitrile (60 mL). After the addition of a solution of the Vilsmeier salt (30 mmol) in acetonitrile (60 mL) dropwise at 0 °C, the reaction mixture was stirred at reflux overnight. The reaction was cooled down and NaOH (1.20 g, 30 mmol) was added. The solvent and NEt$_3$ were evaporated under a vacuum. To complete the deprotonation of the guanidine unit, KOH (20 mL, 50 wt %) was added and the guanidine ligand was extracted with acetonitrile (3 × 50 mL). The collected organic layers were dried with Na$_2$SO$_4$ and activated carbon and the solvent was evaporated under reduced pressure [76,77]. Ligand **L1** was synthesized according to the literature [75]. Ligand **L2** is shown in Scheme 2.

3-((1,3-Dimethylimidazolidine-2-ylidene)amino)-1,2,2-trimethylcyclopentane-1-amine **L2** *(DMEGca,* Scheme 2*).* Yield: 78% (5.58 g, 23.40 mmol). Yellow oil. ^{1}H NMR (400 MHz, CDCl$_3$, 25 °C): δ = 3.70 (dd, *J* = 7.6, 3.7 Hz, 1H), 3.24 (m, 2H), 3.02 (m, 2H), 2.76 (s, 6H), 2.08 (m, 1H), 1.78 (m, 2H), 1.56 (m, 1H), 1.02 (s, 3H), 0.93 (s, 3H), 0.78 (s, 3H) ppm. ^{13}C{^{1}H} NMR (100 MHz, CDCl$_3$, 25 °C): δ = 162.2, 65.3, 49.4, 45.2, 39.9, 31.6, 30.1, 29.1, 24.6, 17.9, 9.2 ppm. IR (NaCl plates): $\tilde{\nu}$ = 2949 {s [ν(C–H$_{aliph}$)]}, 2866 {s [ν(C–H$_{aliph}$)]}, 2463 w, 1701 {vs [ν(C=N$_{gua}$)]}, 1560 (m), 1507 (s), 1442 (s), 1396 (s), 1281 (s), 1200 (m), 1120 (m), 1080 (m), 1031 (s), 957 (m), 931 (m), 906 (w), 858 (w), 762 (m), 721 (w), 649 (m), 581 (s), 473 (vs) cm^{-1}. MS EI(+): *m/z* (%), M = C$_{13}$H$_{26}$N$_4$: 238.6 (1) [C$_{13}$H$_{26}$N$_4$]$^+$, 222.5 (2) [C$_{13}$H$_{24}$N$_3$]$^+$, 206.5 (2) [C$_{12}$H$_{21}$N$_3$]$^+$, 181.5 (6) [C$_{10}$H$_{19}$N$_3$]$^+$, 168.5 (4) [C$_8$H$_{16}$N$_4$]$^+$, 153.4 (8) [C$_8$H$_{15}$N$_3$]$^+$, 114.4 (100) [C$_7$H$_{16}$N]$^+$, 113.4 (55) [C$_7$H$_{15}$N]$^+$, 110.4 (9) [C$_8$H$_{14}$]$^+$. HR-MS EI(+): *m/z* (%), M = C$_{13}$H$_{26}$N$_4$: calc.: 238.2157 [C$_{13}$H$_{26}$N$_4$]$^+$; found: 238.2149 [C$_{13}$H$_{26}$N$_4$]$^+$.
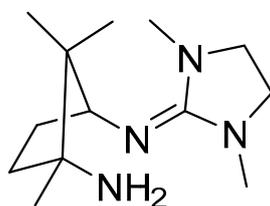
Scheme 2. DMEGca **L2**.

3.6. General Synthesis of Zinc Halide Complexes with Guanidine Ligands

A solution of zinc halide (1 mmol) was dissolved in 2 mL dry THF and a solution of dissolved ligand (1.2 mmol in 2 mL THF) was added to the metal salt solution. Crystals could be obtained by slowly diffusion of diethyl ether. Complex **C1** is shown in Scheme 3, **C2** in Scheme 4 and **C3** in Scheme 5.

2-(3-Amino-2,2,3-trimethylcyclopentyl)-1,1,3,3-tetramethylguanidinedichloridozinc(II) **C1** *([Zn(TMGca)Cl$_2$]*, Scheme 3). Yield: 40% (0.15 g, 0.40 mmol). Colorless crystals. ^{1}H NMR (400 MHz, CDCl$_3$, 25 °C): δ = 3.58 (dd, *J* = 8.3, 1.1 Hz, 1H), 2.97 (s, 6H), 2.84 (s, 6H), 2.38 (m, 1H), 2.15 (m, 2H), 1.86 (m, 1H), 1.23 (s, 3H), 1.16 (s, 3H), 0.96 (s, 3H) ppm. ^{13}C{^{1}H} NMR (100 MHz, CDCl$_3$, 25 °C): δ = 165.0, 70.1, 65.3, 48.7, 40.8, 36.6, 32.3, 27.2, 25.4, 18.6 ppm. IR (KBr): $\tilde{\nu}$ = 3414 (m), 3283 (m), 3269 (m), 3233 (vs), 3155 (s), 3011 (m), 2977 (vs), 2953 (vs), 2929 (vs), 2877 (s), 2798 (m), 1594 {vs [ν(C=N$_{gua}$)]}, 1559 {vs [ν(C=N$_{gua}$)]}, 1524 (vs), 1478 (vs), 1466 (vs), 1408 (vs), 1392 (vs), 1378 (vs), 1371 (vs), 1318 (m), 1295 (m), 1242 (s), 1229 (s), 1168 (s), 1148 (s), 1101 (s), 1079 (s), 1060 (s), 1034 (s), 1023 (s), 1002 (m), 977 (m), 954 (m), 931 (s), 913 (m), 890 (m), 852 (m), 771 (m), 734 (m), 719 (w), 636 (m), 617 (m), 602 (m), 574 (m), 558 (w), 533 (m) cm^{-1}. HR-MS ESI(+): MeCN, *m/z* (%), M = C$_{13}$H$_{28}$Cl$_2$N$_4$Zn: 344.1279 (4) [C$_{12}$^{13}CH$_{28}$^{35}ClN$_4$^{68}Zn]$^+$, 343.1256 (20) [C$_{13}$H$_{28}$^{37}ClN$_4$^{66}Zn; C$_{13}$H$_{28}$^{35}ClN$_4$^{68}Zn]$^+$, 342.1295 (5) [C$_{13}$H$_{28}$^{35}ClN$_4$^{67}Zn; C$_{12}$^{13}CH$_{28}$^{35}ClN$_4$^{66}Zn; C$_{12}$^{13}CH$_{28}$^{37}ClN$_4$^{64}Zn]$^+$, 341.1275 (25) [C$_{13}$H$_{28}$^{35}ClN$_4$^{66}Zn; C$_{13}$H$_{28}$^{37}ClN$_4$^{64}Zn]$^+$, 340.1339 (4) [C$_{12}$^{13}CH$_{28}$^{35}ClN$_4$^{64}Zn]$^+$, 339.1308 (30) [C$_{13}$H$_{28}$^{35}ClN$_4$^{64}Zn]$^+$, 241.2402 (100) [C$_{13}$H$_{29}$N$_4$]$^+$, 224.2135 (20) [C$_{13}$H$_{26}$N$_3$]$^+$; calc.: 339.1294 [C$_{13}$H$_{28}$ClN$_4$Zn]$^+$, 241.2392 [C$_{13}$H$_{29}$N$_4$]$^+$, 224.2127 [C$_{13}$H$_{26}$N$_3$]$^+$.
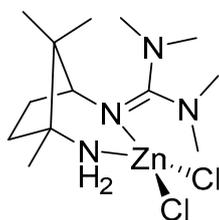
Scheme 3. ([Zn(TMGca)Cl$_2$]) **C1**.

Dichlorido-3-((1,3-Dimethylimidazolidine-2-ylidene)amino)-1,2,2-trimethylcyclopentane-1-aminezinc(II) **C2** *([Zn(DMEGca)Cl$_2$]*, Scheme 4). Yield: 65% (0.24 g, 0.65 mmol). Colorless crystals. ^{1}H NMR (400 MHz, CDCl$_3$, 25 °C): δ = 3.74 (t, *J* = 6.7 Hz, 1H), 3.50 (m, 2H), 3.35 (m, 2H), 3.10 (s, 6H), 2.50 (s, 2H), 2.22 (m, 4H), 1.23 (s, 3H), 1.16 (s, 3H), 0.95 (s, 3H) ppm. ^{13}C{^{1}H} NMR (100 MHz, CDCl$_3$, 25 °C): δ = 163.7, 68.7, 65.5, 49.9, 48.4, 38.5, 36.7, 33.1, 26.4, 25.1, 18.4 ppm. IR (KBr): $\tilde{\nu}$ = 3442 (w), 3233 (m), 3155 (w), 2965 (m), 2872 (w), 1583 {vs [ν(C=N$_{gua}$)]}, 1501 (m), 1466 (m), 1424 (m), 1405 (m), 1382 (w), 1288 (m), 1254 (w), 1168 (w), 1148 (w), 1123 (w), 1102 (w), 1081 (w), 1061 (w), 1040 (w), 992 (vw), 963 (w), 942 (vw), 868 (vw), 807 (vw), 726 (vw) cm^{-1}. HR-MS ESI(+): MeCN, *m/z* (%), M = C$_{13}$H$_{26}$Cl$_2$N$_4$Zn: 365.1527 (25) [C$_{13}$H$_{27}$^{37}ClN$_4$Na^{66}Zn; C$_{13}$H$_{27}$^{35}ClN$_4$Na^{68}Zn]$^+$, 363.1539 (35) [C$_{13}$H$_{27}$^{35}ClN$_4$Na^{66}Zn; C$_{13}$H$_{27}$^{37}ClN$_4$Na^{64}Zn]$^+$, 361.1571 (60) [C$_{13}$H$_{27}$^{35}ClN$_4$Na^{64}Zn]$^+$, 343.1056 (10) [C$_{13}$H$_{26}$^{37}ClN$_4$^{68}Zn]$^+$, 341.1079 (40) [C$_{13}$H$_{26}$^{37}ClN$_4$^{66}Zn; C$_{13}$H$_{26}$^{35}ClN$_4$^{68}Zn]$^+$, 339.1098 (60) [C$_{13}$H$_{26}$^{35}ClN$_4$^{66}Zn; C$_{13}$H$_{26}$^{37}ClN$_4$^{64}Zn]$^+$, 337.1131 (65) [C$_{13}$H$_{26}$^{35}ClN$_4$^{64}Zn]$^+$, 239.2226 (100) [C$_{13}$H$_{27}$N$_4$]$^+$, 222.1961 (55) [C$_{13}$H$_{24}$N$_3$]$^+$; calc.: 361.1108 [C$_{13}$H$_{27}$ClN$_4$NaZn]$^+$, 337.1132 [C$_{13}$H$_{26}$ClN$_4$Zn]$^+$, 239.2230 [C$_{13}$H$_{27}$N$_4$]$^+$, 222.1970 [C$_{13}$H$_{24}$N$_3$]$^+$.
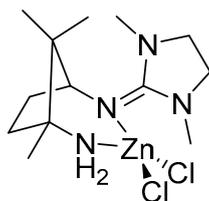
Scheme 4. ([Zn(DMEGca)Cl$_2$]) **C2**.

Dibromido-3-((1,3-Dimethylimidazolidine-2-ylidene)amino)-1,2,2-trimethylcyclopentane-1-aminezinc(II) **C3**
([Zn(DMEGca)Br$_2$]). Yield: 43% (0.20 g, 0.43 mmol). Colorless crystals. ^{1}H NMR (400 MHz, CDCl$_3$,
25 °C): δ = 3.88 (d, *J* = 10.3 Hz, 1H), 3.54 (m, 2H), 3.35 (m, 2H), 3.13 (s, 6H), 2.36 (m, 2H), 2.09 (m, 1H),
1.86 (m, 1H), 1.61 (b. s, 2H), 1.24 (s, 3H), 1.19 (s, 3H), 0.95 (s, 3H) ppm. ^{13}C{^{1}H} NMR (100 MHz, CDCl$_3$,
25°C): δ = 163.8, 68.9, 65.9, 49.9, 48.5, 39.0, 36.6, 33.1, 26.2, 25.1, 18.7 ppm. IR (KBr): $\tilde{\nu}$ = 3279 (m),
3226 (m), 3146 (m), 2960 (m), 2925 (m), 2871 (m), 1586 {vs [ν(C=N$_{gua}$)]}, 1505 (m), 1458 (m), 1421 (m),
1397 (m), 1384 (m), 1291 (m), 1225 (m), 1167 (m), 1147 (m), 1120 (m), 1079 (m), 1034 (m), 966 (w),
945 (w), 859 (vw), 800 (vw), 703 (vw) cm^{-1}. HR-MS ESI(+): MeOH, *m/z* (%), M = C$_{13}$H$_{26}$Cl$_2$N$_4$Zn:
386.1358 (<1) [C$_{13}$H$_{26}$^{81}BrN$_4$^{67}Zn; C$_{12}$^{13}CH$_{26}$^{81}BrN$_4$^{66}Zn; C$_{12}$^{13}CH$_{26}$^{79}BrN$_4$^{68}Zn]$^+$, 385.0566 (<1)
[C$_{13}$H$_{26}$^{81}BrN$_4$^{66}Zn; C$_{13}$H$_{26}$^{79}BrN$_4$^{68}Zn]$^+$, 384.0989 (<1) [C$_{13}$H$_{26}$^{79}BrN$_4$^{67}Zn; C$_{12}$^{13}CH$_{26}$^{79}BrN$_4$^{66}Zn;
C$_{12}$^{13}CH$_{26}$^{81}BrN$_4$^{64}Zn]$^+$, 383.0598 (<1) [C$_{13}$H$_{26}$^{79}BrN$_4$^{66}Zn; C$_{13}$H$_{26}$^{81}BrN$_4$^{64}Zn]$^+$, 382.0663 (<1)
[C$_{12}$^{13}CH$_{26}$^{79}BrN$_4$^{64}Zn]$^+$, 381.0622 (<1) [C$_{13}$H$_{26}$^{79}BrN$_4$^{64}Zn]$^+$, 239.2227 (100) [C$_{13}$H$_{27}$N$_4$]$^+$, 222.1963
(72) [C$_{13}$H$_{24}$N$_3$]$^+$; calc.: 381.0632 [C$_{13}$H$_{26}$BrN$_4$Zn]$^+$, 239.2236 [C$_{13}$H$_{27}$N$_4$]$^+$, 222.1970 [C$_{13}$H$_{24}$N$_3$]$^+$.
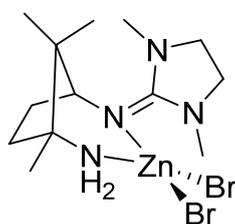
Scheme 5. ([Zn(DMEGca)Br$_2$]) **C3**.

4. Conclusions

Two different monoamine-guanidine hybrid ligands have been synthesized and with zinc halides
three new chiral complexes were obtained. The obtained crystals were fully characterized by X-ray
diffraction, NMR, IR spectroscopy, and mass spectrometry. DFT calculations were performed and are
in good accordance with the solid state structures, whereas the NBO analysis showed a larger negative
charge than the guanidine nitrogen atom. In the solvent-free polymerization of technical *rac*-lactide,
the robust and chiral complexes show great activity and produce colorless polymers at 150 °C.
One selected complex was tested with the addition of a co-initiator and recrystallized lactide to
determine the impact of the co-initiator. We used two different setups: in the polymerization of
technical lactide we used Young tubes in an oil bath (conversion determined via ^{1}H NMR spectroscopy)
and in the polymerization with recrystallized lactide and benzyl alcohol we used a jacketed vessel
and the conversion was determined via FT-IR spectroscopy. The reaction with benzyl alcohol is
several times faster than without. End-group analysis via MALDI-ToF measurements showed that
the co-initiator has opened the lactide monomer and leads to only a small degree of transesterifications.
All complexes show high stability, are robust, and generate colorless polymers. In comparison to
other zinc *N,N*-guanidine complexes, these systems show by far the highest activity in polymerization.
They provide an excellent, sustainable alternative to the conventionally used catalyst, tin octanoate.

References

1. Mekonnen, T.; Mussone, P.; Khalil, H.; Bressler, D. Progress in bio-based plastics and plasticizing modifications. *J. Mater. Chem. A* **2013**, *1*, 13379–13398. [CrossRef]

2. Hayashi, T. Biodegradable polymers for biomedical uses. *Prog. Polym. Sci.* **1994**, *19*, 663–702. [CrossRef]

3. O'Keefe, B.J.; Hillmyer, M.A.; Tolman, W.B. Polymerization of lactide and related cyclic esters by discrete metal complexes. *J. Chem. Soc. Dalton Trans.* **2001**, 2215–2224. [CrossRef]

4. Garlotta, D. A Literature Review of Poly(Lactic Acid). *J. Polym. Environ.* **2001**, *9*, 63–84. [CrossRef]

5. Platel, R.H.; Hodgson, L.M.; Williams, C.K. Biocompatible Initiators for Lactide Polymerization. *Polym. Rev.* **2008**, *48*, 11–63. [CrossRef]

6. Gregory, G.L.; López-Vidal, E.M.; Buchard, A. Polymers from sugars: Cyclic monomer synthesis, ring-opening polymerisation, material properties and applications. *Chem. Comm.* **2017**, *53*, 2198–2217. [CrossRef] [PubMed]

7. Bakewell, C.; White, A.J.P.; Long, N.J.; Williams, C.K. Metal-size influence in Iso-selective lactide polymerization. *Angew. Chem. Int. Ed.* **2014**, *53*, 9226–9230. [CrossRef] [PubMed]

8. Wheaton, C.A.; Hayes, P.G.; Ireland, B.J. Complexes of Mg, Ca and Zn as homogenous catalysts for lactide polymerization. *Dalton Trans.* **2009**, *9226*, 4832. [CrossRef] [PubMed]

9. Dechy-Cabaret, O.; Martin-Vaca, B.; Bourissou, D. Controlled ring-opening polymerization of lactide and glycolide. *Chem. Rev.* **2004**, *104*, 6147–6176. [CrossRef] [PubMed]

10. Auras, R.; Lim, L.T.; Selke, S.E.M.; Tsuji, H. *Poly(Lactic Acid): Synthesis, Structures, Properties, Processing, and Applications*; John Wiley & Sons: Hoboken, NJ, USA, 2010; ISBN 9780470649848.

11. Sudesh, K.; Iwata, T. Sustainability of biobased and biodegradable plastics. *CLEAN-Soil Air Water* **2008**, *36*, 433–442. [CrossRef]

12. Auras, R.; Harte, B.; Selke, S. An Overview of Polylactide as Packaging Materials. *Macromol. Biosci.* **2004**, *4*, 835–864. [CrossRef] [PubMed]

13. Inkinen, S.; Hakkarainen, M.; Albertsson, A.C.; Södergård, A. From lactic acid to poly(lactic acid) (PLA): Characterization and analysis of PLA and its precursors. *Biomacromolecules* **2011**, *12*, 523–532. [CrossRef] [PubMed]

14. Thomas, C.M. Stereocontrolled ring-opening polymerization of cyclic esters: Synthesis of new polyester microstructures. *Chem. Soc. Rev.* **2010**, *39*, 165–173. [CrossRef] [PubMed]

15. Miller, S.A. Sustainable polymers: Opportunities for the next decade. *ACS Macro Lett.* **2013**, *2*, 550–554. [CrossRef]

16. Zhu, Y.; Romain, C.; Williams, C.K. Sustainable polymers from renewable resources. *Nature* **2016**, *540*, 354–362. [CrossRef] [PubMed]

17. Chisholm, M.H.; Patmore, N.J.; Zhou, Z. Concerning the relative importance of enantiomorphic site vs. chain end control in the stereoselective polymerization of lactides: Reactions of (*R*,*R*-salen)-and (*S*,*S*-salen)-aluminium alkoxides LAlOCH$_2$R complexes (R = CH$_3$ and S–CHMeCl). *Chem. Commun.* **2005**, 127–129. [CrossRef] [PubMed]

18. Bonnet, F.; Cowley, A.R.; Mountford, P. Lanthanide Borohydride Complexes Supported by Diaminobis(phenoxide) Ligands for the Polymerization of ε-Caprolactone and L- and *rac*-Lactide. *Inorg. Chem.* **2005**, *44*, 9046–9055. [CrossRef] [PubMed]

19. Zhong, Z.Y.; Dijkstra, P.J.; Feijen, J. [(salen)Al]-Mediated, Controlled and Stereoselective Ring-Opening Polymerization of Lactide in Solution and without Solvent: Synthesis of Highly Isotactic Polylactide Stereocopolymers from Racemic D,L-Lactide. *Angew. Chem.* **2002**, *114*, 4692–4695. [CrossRef]

20. Zhong, Z.Y.; Dijkstra, P.J.; Feijen, J. Controlled and stereoselective polymerization of lactide: Kinetics, selectivity, and microstructures. *J. Am. Chem. Soc.* **2003**, *125*, 11291–11298. [CrossRef] [PubMed]

21. Spassky, N.; Wisniewski, M.; Pluta, C.; Le Borgne, A. Highly stereoselective polymerization of *rac*-(D,L)-lactide with a chiral Schiff's base/aluminium alkoxide initiator. *Macromol. Chem. Phys.* **1996**, *197*, 2627–2637. [CrossRef]

22. Ovitt, T.M.; Coates, G.W. Stereochemistry of lactide polymerization with chiral catalysts: New opportunities for stereocontrol using polymer exchange mechanisms. *J. Am. Chem. Soc.* **2002**, *124*, 1316–1326. [CrossRef] [PubMed]

23. Jones, M.D.; Davidson, M.G.; Keir, C.G.; Hughes, L.M.; Mahon, M.F.; Apperley, D.C. Zinc(II) Homogeneous and Heterogeneous Species and their Application for the Ring-Opening Polymerisation of *rac*-Lactide. *Eur. J. Inorg. Chem.* **2009**, 635–642. [CrossRef]

24. Whitelaw, E.L.; Davidson, M.G.; Jones, M.D. Group 4 salalen complexes for the production and degradation of polylactide. *Chem. Commun.* **2011**, *47*, 10004–10006. [CrossRef] [PubMed]

25. Stopper, A.; Press, K.; Okuda, J.; Goldberg, I.; Kol, M. Zirconium Complexes of Phenylene-Bridged {ONSO} Ligands: Coordination Chemistry and Stereoselective Polymerization of *rac*-Lactide. *Inorg. Chem.* **2014**, *53*, 9140–9150. [CrossRef] [PubMed]

26. Sauer, A.; Kapelski, A.; Fliedel, C.; Dagorne, S.; Kol, M.; Okuda, J. Switching the Lactide Polymerization Activity of a Cerium Complex by Redox Reactions. *Dalton Trans.* **2013**, *42*, 9007–9023. [CrossRef] [PubMed]

27. Hermans, C.; Rong, W.; Spaniol, T.P.; Okuda, J. Lanthanum complexes containing a bis(phenolate) ligand with a ferrocene-1,1′-diyldithio backbone: Synthesis, characterization, and ring-opening polymerization of *rac*-lactide. *Dalton Trans.* **2016**, *45*, 8127–8133. [CrossRef] [PubMed]

28. Bakewell, C.; White, A.J.P.; Long, N.J.; Williams, C.K. Scandium and yttrium phosphasalen complexes as initiators for ring-opening polymerization of cyclic esters. *Inorg. Chem.* **2015**, *54*, 2204–2212. [CrossRef] [PubMed]

29. Stanford, M.J.; Dove, A.P. Stereocontrolled ring-opening polymerisation of lactide. *Chem. Soc. Rev.* **2010**, *39*, 486–494. [CrossRef] [PubMed]

30. Chisholm, M.; Eilerts, N.W.; Huffman, J.C.; Iyer, S.S.; Pacold, M.; Phomphrai, K. Molecular Design of Single-Site Metal Alkoxide Catalyst Precursors for Ring-Opening Polymerization Reactions Leading to Polyoxygenates. 1. Polylactide Formation by Achiral and Chiral Magnesium and Zinc Alkoxides, (η^3-L)MOR, Where L = Trispyrazolyl- and Trisindazolylborate Ligands. *J. Am. Chem. Soc.* **2000**, *122*, 11845–11854. [CrossRef]

31. Chisholm, M.H.; Gallucci, J.; Phomphrai, K. Lactide polymerization by well-defined calcium coordination complexes: Comparisons with related magnesium and zinc chemistry. *Chem. Commun.* **2003**, 48–49. [CrossRef]

32. Poirier, V.; Roisnel, T.; Carpentier, J.-F.; Sarazin, Y. Zinc and magnesium complexes supported by bulky multidentate amino-ether phenolate ligands: Potent pre-catalysts for the immortal ring-opening polymerisation of cyclic esters. *Dalton Trans.* **2011**, *40*, 523–534. [CrossRef] [PubMed]

33. Chamberlain, B.M.; Cheng, M.; Moore, D.R.; Ovitt, T.M.; Lobkovsky, E.B.; Coates, G.W. Polymerization of lactide with zinc and magnesium β-diiminate complexes: Stereocontrol and mechanism. *J. Am. Chem. Soc.* **2001**, *123*, 3229–3238. [CrossRef] [PubMed]

34. Cheng, M.; Attygalle, A.B.; Lobkovsky, E.B.; Coates, G.W. Single-Site Catalysts for Ring-Opening Polymerization: Synthesis of Heterotactic Poly(lactic acid) from *rac*-Lactide. These homogeneous, molecular compounds have the general formula LnMR, where Ln is a ligand set that remains attached to and thus. *J. Am. Chem. Soc.* **1999**, *121*, 11583–11584. [CrossRef]

35. Dove, A.P.; Gibson, V.C.; Marshall, E.L.; White, A.J.P.; Williams, D.J. Magnesium and zinc complexes of a potentially tridentate β-diketiminate ligand. *Dalton Trans.* **2004**, 570–578. [CrossRef] [PubMed]

36. Chisholm, M.H.; Gallucci, J.C.; Phomphrai, K. Comparative study of the coordination chemistry and lactide polymerization of alkoxide and amide complexes of zinc and magnesium with a β-diiminato ligand bearing ether substituents. *Inorg. Chem.* **2005**, *44*, 8004–8010. [CrossRef] [PubMed]

37. Gerling, K.A.; Rezayee, N.M.; Rheingold, A.L.; Green, D.B.; Fritsch, J.M. Synthesis and structures of bis-ligated zinc complexes supported by tridentate ketoimines that initiate L-lactide polymerization. *Dalton Trans.* **2014**, *43*, 16498–16508. [CrossRef] [PubMed]

38. Chen, Y.-H.; Chen, Y.-J.; Tseng, H.-C.; Lian, C.-J.; Tsai, H.-Y.; Lai, Y.-C.; Hsu, S.C.N.; Chiang, M.Y.; Chen, H.Y. Comparing L-lactide and ε-caprolactone polymerization by using aluminum complexes bearing ketimine ligands: Steric, electronic, and chelating effects. *RSC Adv.* **2015**, *5*, 100272–100280. [CrossRef]

39. Scheiper, C.; Dittrich, D.; Wölper, C.; Bläser, D.; Roll, J.; Schulz, S. Synthesis, Structure, and Catalytic Activity of Tridentate, Base-Functionalized β-Ketiminate Zinc Complexes in Ring-Opening Polymerization of Lactide. *Eur. J. Inorg. Chem.* **2014**, 2230–2240. [CrossRef]

40. Scheiper, C.; Schulz, S.; Wölper, C.; Bläser, D.; Roll, J. Synthesis and single crystal X-ray structures of cationic zinc β-diketiminate complexes. *Z. Anorg. Allg. Chem.* **2013**, *639*, 1153–1159. [CrossRef]

41. Scheiper, C.; Wölper, C.; Bläser, D.; Roll, J.; Schulz, S. Syntheses, solid-state structures and catalytic activity of zinc carboxylate complexes in lactide polymerization. *Z. Naturforsch.* **2014**, *69*, 1365–1374. [CrossRef]

42. Jones, M.D.; Hancock, S.L.; McKeown, P.; Schäfer, P.M.; Buchard, A.; Thomas, L.H.; Mahon, M.F.; Lowe, J.P. Zirconium complexes of bipyrrolidine derived salan ligands for the isoselective polymerisation of *rac*-lactide. *Chem. Commun.* **2014**, *50*, 15967–15970. [CrossRef] [PubMed]

43. Jones, M.D.; Brady, L.; McKeown, P.M.; Buchard, A.; Schäfer, P.M.; Thomas, L.H.; Mahon, M.F.M.; Woodman, T.J.; Lowe, J.P. Metal influence on the iso- and hetero-selectivity of complexes of bipyrrolidine derived Salan ligands for the polymerisation of *rac*-lactide. *Chem. Sci.* **2015**, 5034–5039. [CrossRef] [PubMed]

44. Kirk, S.M.; Quilter, H.C.; Buchard, A.; Thomas, L.H.; Kociok-Kohn, G.; Jones, M.D. Monomeric and dimeric Al(III) complexes for the production of polylactide. *Dalton Trans.* **2016**, *45*, 13846–13852. [CrossRef] [PubMed]

45. Wang, X.; Zhao, K.-Q.; Al-Khafaji, Y.; Mo, S.; Prior, T.J.; Elsegood, M.R.; Redshaw, C. Organoaluminium Complexe Derived from Anilines or Schiff Bases for the Ring-Opening Polymerization of ε-Caprolactone, δ-Valerolactone and *rac*-Lactide. *Eur. J. Inorg. Chem.* **2017**, 1951–1965. [CrossRef]

46. Yang, W.; Zhao, K.-Q.; Prior, T.J.; Hughes, D.L.; Arbaoui, A.; Elsegood, M.R.J.; Redshaw, C. Structural studies of Schiff-base [2 + 2] macrocycles derived from 2,2′-oxydianiline and the ROP capability of their organoaluminium complexes. *Dalton Trans.* **2016**, *45*, 11990–12005. [CrossRef] [PubMed]

47. Al-Khafaji, Y.F.; Elsegood, M.R.J.; Frese, J.W.A.; Redshaw, C. Ring opening polymerization of lactides and lactones by multimetallic alkyl zinc complexes derived from the acids $Ph_2C(X)CO_2H$ (X = OH, NH_2). *RSC Adv.* **2017**, *7*, 4510–4517. [CrossRef]

48. Bakewell, C.; Fateh-Iravani, G.; Beh, D.W.; Myers, D.; Tabthong, S.; Hormnirun, P.; White, A.J.P.; Long, N.; Williams, C.K. Comparing a series of 8-quinolinolato complexes of aluminium, titanium and zinc as initiators for the ring-opening polymerization of *rac*-lactide. *Dalton Trans.* **2015**, *44*, 12326–12337. [CrossRef] [PubMed]

49. Thevenon, A.; Romain, C.; Bennington, M.S.; White, A.J.P.; Davidson, H.J.; Brooker, S.; Williams, C.K. Dizinc Lactide Polymerization Catalysts: Hyperactivity by Control of Ligand Conformation and Metallic Cooperativity. *Angew. Chem.* **2016**, *128*, 8822–8827. [CrossRef]

50. Nijenhuis, A.J.; Grijpma, D.W.; Pennings, A.J. Lewis acid catalyzed polymerization of L-lactide. Kinetics and mechanism of the bulk polymerization. *Macromolecules* **1992**, *25*, 6419–6424. [CrossRef]

51. Leenslag, J.W.; Pennings, A.J. Synthesis of high-molecular-weight poly(lactide) initiated with tin 2-ethylhexanoate. *Makromol. Chem.* **1987**, *188*, 1809–1814. [CrossRef]

52. Degée, P.; Dubois, P.; Jérôme, R.; Jacobsen, S.; Fritz, H.-G. New catalysis for fast bulk ring-opening polymerization of lactide monomers. *Macromol. Symp.* **1999**, *144*, 289–302. [CrossRef]

53. Stjerndahl, A.; Finne-Wistrand, A.; Albertsson, A.-C.; Bäckesjö, C.M.; Lindgren, U. Minimization of residual tin in the controlled Sn(II) octoate-catalyzed polymerization of ε-caprolactone. *J. Biomed. Mater. Res. Part A* **2008**, *87*, 1086–1091. [CrossRef] [PubMed]

54. Sun, H.; Ritch, J.S.; Hayes, P.G. Toward stereoselective lactide polymerization catalysts: Cationic zinc complexes supported by a chiral phosphinimine scaffold. *Inorg. Chem.* **2011**, *50*, 8063–8072. [CrossRef] [PubMed]

55. Wheaton, C.A.; Hayes, P.G. Cationic zinc complexes: A new class of catalyst for living lactide polymerization at ambient temperature. *Chem. Commun.* **2010**, *46*, 8404–8406. [CrossRef] [PubMed]

56. Wheaton, C.A.; Hayes, P.G. Cationic organozinc complexes of a bis(phosphinimine) pincer ligand: Synthesis, structural and polymerization studies. *Dalton Trans.* **2010**, *39*, 3861–3869. [CrossRef] [PubMed]

57. Ireland, B.J.; Wheaton, C.A.; Hayes, P.G. Cationic Organomagnesium Complexes as Highly Active Initiators for the Ring-Opening Polymerization of ε-Caprolactone. *Organometallics* **2010**, *29*, 1079–1084. [CrossRef]

58. Wheaton, C.A.; Ireland, B.J.; Hayes, P.G. Activated zinc complexes supported by a neutral, phosphinimine-containing ligand: Synthesis and efficacy for the polymerization of lactide. *Organometallics* **2009**, *28*, 1282–1285. [CrossRef]

59. Kwon, K.S.; Nayab, S.; Jeong, J.H. Synthesis, characterisation and X-ray structures of zinc(II) complexes bearing camphor-based iminopyridines as pre-catalysts for heterotactic-enriched polylactide from *rac*-lactide. *Polyhedron* **2015**, *85*, 615–620. [CrossRef]

60. Kwon, K.S.; Nayab, S.; Jeong, J.H. Synthesis, characterisation and X-ray structure of Cu(II) and Zn(II) complexes bearing *N*,*N*-dimethylethylenamine-camphorylimine ligands: Application in the polymerisation of *rac*-lactide. *Polyhedron* **2017**, 23–29. [CrossRef]

61. Cushion, M.G.; Mountford, P. Cationic and charge-neutral calcium tetrahydroborate complexes and their use in the controlled ring-opening polymerisation of *rac*-lactide. *Chem. Commun.* **2011**, *47*, 2276–2278. [CrossRef] [PubMed]

62. Jensen, T.R.; Breyfogle, L.E.; Hillmyer, M.A.; Tolman, W.B. Stereoelective polymerization of D,L-lactide using *N*-heterocyclic carbene based compounds. *Chem. Commun.* **2004**, 2504–2505. [CrossRef] [PubMed]

63. Jensen, T.R.; Schaller, C.P.; Hillmyer, M.A.; Tolman, W.B. Zinc *N*-heterocyclic carbene complexes and their polymerization of D,L-lactide. *J. Organomet. Chem.* **2005**, *690*, 5881–5891. [CrossRef]

64. Liu, J.; Ma, H. Aluminum complexes with bidentate amido ligands: Synthesis, structure and performance on ligand-initiated ring-opening polymerization of *rac*-lactide. *Dalton Trans.* **2014**, *43*, 9098. [CrossRef] [PubMed]

65. Dos Santos Vieira, I.; Herres-Pawlis, S. Lactide polymerisation with complexes of neutral *N*-donors-new strategies for robust catalysts. *Eur. J. Inorg. Chem.* **2012**, 765–774. [CrossRef]

66. Neuba, A.; Herres-Pawlis, S.; Seewald, O.; Börner, J.; Heuwing, A.J.; Flörke, U.; Henkel, G. A Systematic Study on the Coordination Properties of the Guanidine. *Z. Anorg. Allg. Chem.* **2010**, *636*, 2641–2649. [CrossRef]

67. Reinmuth, M.; Walter, P.; Enders, M.; Kaifer, E.; Himmel, H.J. Zinc Halide and Alkylzinc Complexes of a Neutral Doubly Base-Stabilized Diborane(4). *Eur. J. Inorg. Chem.* **2011**, 83–90. [CrossRef]

68. Stanek, J.; Rösener, T.; Metz, A.; Mannsperger, J.; Hoffmann, A.; Herres-Pawlis, S. *Topics in Heterocyclic Chemistry*; Springer: Basel, Switzerland, 2015; ISSN 15334880.

69. Metz, A.; Plothe, R.; Glowacki, B.; Koszalkowski, A.; Scheckenbach, M.; Beringer, A.; Rösener, T.; Michalis de Vasconcellos, J.; Haase, R.; Flörke, U.; et al. Zinc Chloride Complexes with Aliphatic and Aromatic Guanidine Hybrid Ligands and their Activity in the Ring-Opening Polymerisation of D,L-Lactide. *Eur. J. Inorg. Chem.* **2016**, 4974–4987. [CrossRef]

70. Metz, A.; McKeown, P.; Esser, B.; Gohlke, C.; Kröckert, K.; Laurini, L.; Scheckenbach, M.; McCormick, S.N.; Oswald, M.; Hoffmann, A.; et al. Zn(II) chloride complexes with novel aliphatic, chiral bisguanidine ligands as catalysts in the ring-opening polymerisation of *rac*-lactide using FT-IR spectroscopy in bulk. *Eur. J. Inorg. Chem.* **2017**. [CrossRef]

71. Schäfer, P.M.; Fuchs, M.; Ohligschläger, A.; Rittinghaus, R.; McKeown, P.; Akin, E.; Schmidt, M.; Hoffmann, A.; Liauw, M.A.; Jones, M.D.; et al. Fast and robust: Novel highly active N,O zinc guanidine catalysts for the ring-opening polymerisation of lactide. *ChemSusChem* **2017**. [CrossRef]

72. Börner, J.; Flörke, U.; Huber, K.; Döring, A.; Kuckling, D.; Herres-Pawlis, S. Lactide polymerisation with air-stable and highly active zinc complexes with guanidine-pyridine hybrid ligands. *Chem. Eur. J.* **2009**, *15*, 2362–2376. [CrossRef] [PubMed]

73. Börner, J.; dos Santos Vieira, I.; Pawlis, A.; Döring, A.; Kuckling, D.; Herres-Pawlis, S. Mechanism of the living lactide polymerization mediated by robust zinc guanidine complexes. *Chem. Eur. J.* **2011**, *17*, 4507–4512. [CrossRef] [PubMed]

74. Börner, J.; Herres-Pawlis, S.; Flörke, U.; Huber, K. [Bis(guanidine)] Zinc Complexes and their Application in Lactide Polymerisation. *Eur. J. Inorg. Chem.* **2007**, 5645–5651. [CrossRef]

75. Wern, M.; Ortmeyer, J.; Josephs, P.; Schneider, T.; Neuba, A.; Henkel, G.; Schindler, S. Syntheses, characterization, and reactivity of copper complexes with camphor-like tetramethylguanidine ligands. *Inorg. Chim. Acta* **2017**. [CrossRef]

76. Herres-Pawlis, S.; Neuba, A.; Seewald, O.; Seshadri, T.; Egold, H.; Flörke, U.; Henkel, G. A library of peralkylated bis-guanidine ligands for use in biomimetic coordination chemistry. *Eur. J. Org. Chem.* **2005**, 4879–4890. [CrossRef]

77. Kantlehner, W.; Haug, E.; Mergen, W.W.; Speh, P.; Maier, T.; Kapassakalidis, J.J.; Bräuner, H.J.; Hagen, H. Orthoamide, XL. Herstellung von 1,1,2,3,3-pentasubstituierten und 1,1,2,2,3,3-hexasubstituierten Guanidiniumsalzen sowie von 1,1,2,3,3-PentaalkyIguanidinen. *Liebigs Ann. Chem. Weinheim* **1984**, 108–126. [CrossRef]

78. Rösener, T.; Bienemann, O.; Sigl, K.; Schopp, N.; Schnitter, F.; Flörke, U.; Hoffmann, A.; Döring, A.; Kuckling, D.; Herres-Pawlis, S. A Comprehensive Study of Copper Guanidine Quinoline Complexes: Predicting the Activity of Catalysts in ATRP with DFT. *Chem. Eur. J.* **2016**, *22*, 13550–13562. [CrossRef] [PubMed]

79. Yang, L.; Powell, D.R.; Houser, R.P. Structural variation in copper(I) complexes with pyridylmethylamide ligands: Structural analysis with a new four-coordinate geometry index, τ_4. *Dalton Trans.* **2007**, 955–964. [CrossRef] [PubMed]

80. Raab, V.; Harms, K.; Sundermeyer, J.; Kovačević, B.; Maksić, Z.B. 1,8-Bis(dimethylethyleneguanidino)-naphthalene: Tailoring the Basicity of Bisguanidine "Proton Sponges" by Experiment and Theory. *J. Org. Chem.* **2003**, *68*, 8790–8797. [CrossRef] [PubMed]

81. Staroverov, V.N.; Scuseria, G.E.; Tao, J.; Perdew, J.P. Comparative assessment of a new nonempirical density functional: Molecules and hydrogen-bonded complexes. *J. Chem. Phys.* **2009**, 12129–12137. [CrossRef]

82. Weigend, F.; Ahlrichs, R. Balanced basis sets of split valence, triple zeta valence and quadruple zeta valence quality for H to Rn: Design and assessment of accuracy. *Phys. Chem. Chem. Phys.* **2005**, *7*, 3297–3305. [CrossRef] [PubMed]

83. Hoffmann, A.; Grunzke, R.; Herres-Pawlis, S. Insights into the influence of dispersion correction in the theoretical treatment of guanidine-quinoline copper(I) complexes. *J. Comput. Chem.* **2014**, *35*, 1943–1950. [CrossRef] [PubMed]

84. Goerigk, L.; Grimme, S. A thorough benchmark of density functional methods for general main group thermochemistry, kinetics, and noncovalent interactions. *Phys. Chem. Chem. Phys.* **2011**, *13*, 6670. [CrossRef] [PubMed]

85. Grimme, S.; Ehrlich, S.; Goerigk, L. Effect of the damping function in dispersion corrected density functional theory. *J. Comput. Chem.* **2011**, 1456–1465. [CrossRef] [PubMed]

86. Weinhold, F.; Landis, C. *Valency and Bonding—A Natural Bond Orbital Donor-Acceptor Perspective*; Cambridge University: New York, NY, USA, 2005; ISBN 978-0521831284.

87. Glendening, E.D.; Landis, C.R.; Weinhold, F. NBO 6.0: Natural Bond Orbital Analysis Program. *J. Comput. Chem.* **2013**, *34*, 1429–1437. [CrossRef] [PubMed]

88. Glendening, E.D.; Badenhoop, J.K.; Reed, A.E.; Carpenter, J.E.; Bohmann, J.A.; Morales, C.M.; Landis, C.R.; Weinhold, F. *NBO 6.0*; Theoretical Chemistry Institute, University of Wisconsin: Madison, WI, USA, 2013.

89. Chuck, C.; Davidson, M.G.; Gobius du Sart, G.; Ivanova-Mitseva, P.K.; Kociok-Köhn, G.I.; Manton, L.B. Synthesis and structural characterization of group 4 metal alkoxide complexes of *N,N,N′,N′*-tetrakis(2-hydroxyethyl)ethylenediamine and their use as initiators in the ring-opening polymerization (ROP) of *rac*-lactide under industrially relevant conditions. *Inorg. Chem.* **2013**, *52*, 10804–10811. [CrossRef] [PubMed]

90. Leonhard, L.; Lygo, B.; Procter, G. *Praxis in der Organischen Chemie*; VCH Verlagsgesellschaft: Weinheim, Germany, 1996; ISBN 978-3-527-33250-2.

91. Bruker AXS Inc. *SAINT V8.37A*; Bruker AXS Inc.: Madison, WI, USA, 2008.

92. Bruker AXS Inc. *SADABS-2008/1*; Bruker AXS Inc.: Madison, WI, USA, 2008.

93. Bruker AXS Inc. *XPREP*; Version 5.1/NT; Bruker AXS Inc.: Madison, WI, USA, 2007.

94. Sheldrick, G.M. Phase annealing in *SHELX*-90: Direct methods for larger structures. *Acta Crystallogr. Sect. A* **1990**, *46*, 467–473. [CrossRef]

95. Hübschle, C.B.; Sheldrick, G.M.; Dittrich, B. ShelXle: A Qt graphical user interface for *SHELXL*. *J. Appl. Cryst.* **2011**, *44*, 1281–1284. [CrossRef] [PubMed]

96. Frisch, M.J.; Trucks, G.W.; Schlegel, H.B.; Scuseria, G.E.; Robb, M.A.; Cheeseman, J.R.; Scalmani, G.; Barone, V.; Mennucci, B.; Petersson, G.A.; et al. *Expanding the Limits of Computational Chemistry*; Gaussian 09 Revision E.01; Gaussian, Inc.: Wallingford, CT, USA, 2009.

97. Marenich, A.V.; Cramer, C.J.; Truhlar, D.G. Universal solvation model based on solute electron density and on a continuum model of the solvent defined by the bulk dielectric constant and atomic surface tensions. *J. Phys. Chem. B* **2009**, 6378–6396. [CrossRef] [PubMed]

98. Krüger, J.; Grunzke, R.; Gesing, S.; Breuers, S.; Brinkmann, A.; de la Garza, L.; Kohlbacher, O.; Kruse, M.; Nagel, W.; Packschies, L.; et al. The MoSGrid Science Gateway: A Complete Solution for Molecular Simulations. *J. Chem. Theory Comput.* **2014**, *10*, 2232–2245. [CrossRef] [PubMed]

99. Herres-Pawlis, S.; Hoffmann, A.; Balasko, A.; Kacsuk, P.; Birkenheuer, G.; Brinkmann, A.; de la Garza, L.; Krüger, J.; Gesing, S.; Grunzke, R.; et al. Quantum chemical meta-workflows in MoSGrid. *Concurr. Comput. Pract. Exp.* **2015**, *27*, 344–357. [CrossRef]

100. Gesing, S.; Grunzke, R.; Krüger, J.; Birkenheuer, G.; Wewior, M.; Schäer, P.; Schuller, B.; Schuster, J.; Herres-Pawlis, S.; Breuers, S.; et al. A Single Sign-On Infrastructure for Science Gateways on a Use Case for Structural Bioinformatic. *J. Grid Comput.* **2012**, *10*, 769–790. [CrossRef]